

Discovery of 1RXS J171824.2–402934 as an X-ray burster

R.G. Kaptein¹, J.J.M. in 't Zand¹, E. Kuulkers^{1,2}, F. Verbunt², J. Heise¹, and R. Cornelisse^{1,2}

¹ Space Research Organization Netherlands, Sorbonnelaan 2, NL - 3584 CA Utrecht, the Netherlands

² Astronomical Institute, Utrecht University, P.O. Box 80000, NL - 3508 TA Utrecht, the Netherlands

Received, accepted

Abstract. We report the first-time detection of a type-I X-ray burst from a position that is consistent with that of 1RXS J171824.2–402934. The detection was made on Sep 23, 1996, with the Wide Field Cameras on board the BeppoSAX satellite. The burst had a peak intensity of 1.3 Crab units in 2 to 28 keV and is relatively long (at least 3.5 min). Analysis of the burst gives clear evidence for photospheric radius expansion. Assuming the peak luminosity to be close to the Eddington limit, standard burst parameters and taking into account gravitational redshift effects, the distance to the source is approximately 6.5 kpc. No other bursts from this source have been observed during the rest of the WFC observations. The detection of a type-I burst implies that 1RXS J171824.2–402934 in all likelihood is a low-mass X-ray binary where the compact object is a neutron star.

Key words: stars: individual: 1RXS J171824.2–402934 – stars: neutron – X-rays: bursts

1. Introduction

1RXS J171824.2–402934 was first detected during the ROSAT All-Sky Survey (Voges et al. 1999) on September 2, 1990, when it had a count rate of 0.157 c s^{-1} (0.1–2.4 keV) in the Position Sensitive Proportional Counter. The spectral hardness of the source was high, suggesting an X-ray binary (Motch et al. 1998). Two pointed observations were done with ROSAT in March and September 1994 with net exposure times of 790 and 2479 seconds respectively using the High-Resolution Imager. The count rates were 0.048 and 0.019 c s^{-1} respectively. The position was determined to be $\alpha_{2000.0} = 17^{\text{h}}18^{\text{m}}24.13^{\text{s}}$, $\delta_{2000.0} = -40^{\circ}29'30''.4$ with a 90% confidence error radius of $15''.7$ (Motch et al. 1998). Motch et al. searched for the optical counterpart, but were unable to identify one.

We here present the analysis of a short flare that was observed from the same sky position with the Wide Field Cameras (WFCs) on the BeppoSAX satellite in September

1996 and explain it within the framework of thermonuclear flashes on neutron stars.

2. Observations

The WFCs (Jager et al. 1997) are two identical coded aperture cameras on board the BeppoSAX satellite (Boella et al. 1997), which was launched on April 30, 1996. Each camera consists of a coded mask and a position-sensitive proportional counter. The field of view is $40^{\circ} \times 40^{\circ}$ (full width to zero response), the angular resolution $5'$ and the source location accuracy is generally better than $1'$. The energy range is 2 to 28 keV with an energy resolution of 18% at 6 keV. The on-axis detection threshold is of the order of a few mCrab in 10^5 s , and varies as a function of the total flux contained in the field of view. The WFCs are particularly suitable for the study of fast transient X-ray phenomena at unexpected sky positions, thanks to the large coverage of the sky in combination with good angular resolution.

In 1996 the Galactic center was targeted by the WFCs for 22 days during August 21 to October 29. The source reported here is $13^{\circ}.4$ from the Galactic center, well within the field of view. The net exposure time of the source during this period is 550 ks.

3. Detection and position

One of the WFCs detected the X-ray flare on Sep 23.313, 1996 (UT, or MJD 50349.313) at a position of $\alpha_{2000.0} = 17^{\text{h}}18^{\text{m}}23.6^{\text{s}}$, $\delta_{2000.0} = -40^{\circ}29'46''$. The error radius is $0'.9$ (at the 99% confidence level). 1RXS J171824.2–402934 is $0'.3$ from this position and well within the WFC error circle. The nearest other known X-ray source is 1RXS J171935.6–410054, at an angular distance of $36'$. We conclude that the flare is from 1RXS J171824.2–402934.

The WFC data do not show a detection of the persistent emission of 1RXS J171824.2–402934 over any part of the 1996 observations. The upper limit is $6 \times 10^{-11} \text{ erg cm}^{-2}\text{s}^{-1}$ (2–10 keV), over all the 1996 data. The flux measured with ROSAT and translated to 2–10 keV numbers (assuming a power-law spectrum with a photon index

of 2.1 and $N_{\text{H}} = 9.2 \times 10^{21} \text{ cm}^{-2}$, see below) varies from $1 \times 10^{-11} \text{ erg cm}^{-2}\text{s}^{-1}$ (September 1990) to $9 \times 10^{-12} \text{ erg cm}^{-2}\text{s}^{-1}$ (March 1994) to $4 \times 10^{-12} \text{ erg cm}^{-2}\text{s}^{-1}$ (September 1994). The uncertainty of these numbers is large due to the lack of knowledge of the persistent spectrum, and we estimate it to be a factor of 2.

Unfortunately, the flare occurred close to earth occultation. Model calculations predict that the flux in the heaviest degraded calibrated WFC-channel experiences absorption by less than 10% as long as the direction is higher than 145 km above the earth limb. 1RXS J171824.2–402934 sets behind the earth 209 s after the flare onset, while the height of 145 km was reached after 135 s.

4. Data analysis

The light curve of the flare is shown in various passbands in the top panels of Fig. 1. The rise time to the peak level is quick (~ 6 s), while the decay is comparatively slow ($\gtrsim 200$ s). During the first minute the flux is approximately constant at a peak level of $2.6 \text{ ct s}^{-1}\text{cm}^{-2}$ or 1.3 Crab units (2–28 keV). The flare starts off at a relatively high hardness ratio (see Fig. 1d), after which it decreases during ~ 20 s, followed by an increase over ~ 70 s to a similar peak value. Finally, it decreases again for the remainder of the flare.

We modeled the flare spectrum with black-body radiation, thermal bremsstrahlung and a power-law function, all subjected to interstellar absorption. We used the data of the first and brightest 60 s of the flare. This duration is a compromise between obtaining sufficient statistics for a meaningful model comparison, and limiting the spectral change within the data set as suggested by the hardness ratio. The best fits of the three models resulted in χ^2_{r} values of 0.72, 2.52 and 4.59 respectively, all for 26 degrees of freedom. We conclude that black-body radiation is the best description of the data. During later parts of the flare, black-body fits also gave the best results. Two examples of burst spectra are shown in Fig. 2.

We carried out time-resolved spectroscopy by resolving the flare in 20 time intervals, generating spectra for those intervals, and fitting a black-body model with absorption to each of those spectra. We kept the absorbing column N_{H} tied to a single value over all intervals up to the point where the source direction enters the earth atmosphere (indicated by the dotted line in Fig. 1) and left it tied again in the group of spectra after that. The results of the fit for the black body temperature kT_{bb} and radius R_{bb} at an assumed distance of 10 kpc are presented in Figs. 1e and f. The errors in the fit parameters are single-parameter 1σ uncertainties. The absorbing column over all intervals up to earth-atmosphere entry was found to be $(3.1 \pm 1.3) \times 10^{22} \text{ cm}^{-2}$ (90% confidence). This compares to $9.2 \times 10^{21} \text{ cm}^{-2}$ as found from interpolation of HI maps (Dickey & Lockman 1990), so is 3 times as high at about

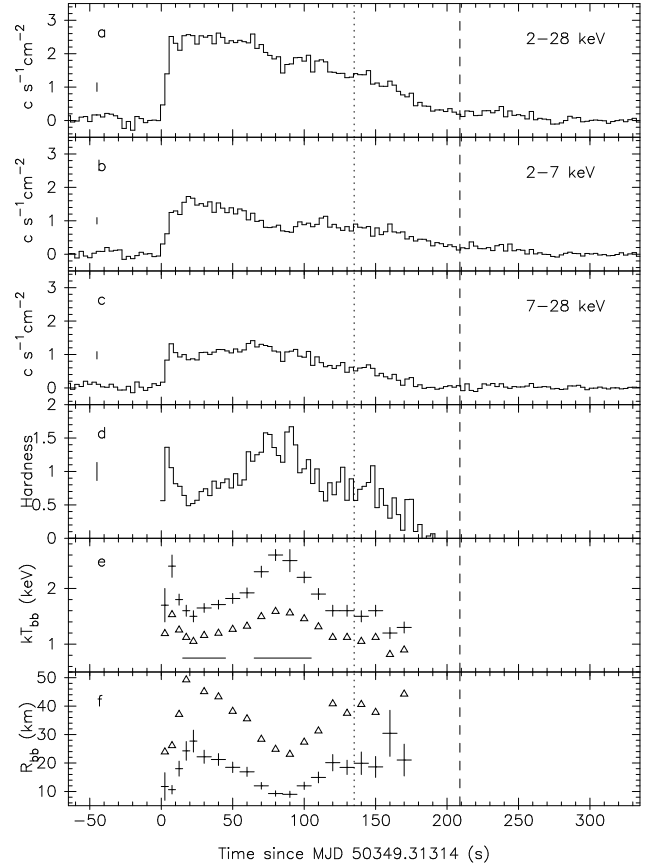


Fig. 1. **a**, **b** and **c** show the light curve in the 2–28 keV, 2–7 keV and 7–28 keV energy bands. **d** shows the hardness ratio during the flare. The hardness ratio is the ratio of the count rates in the 7–28 keV and the 2–7 keV bands. The bin time for **a–d** is 3 s, and typical error bars of length 1σ for respectively the fluxes and the hardness are indicated at the left. The crosses in **e** and **f** show the black-body temperature kT_{bb} (in keV) and the effective black-body radius R_{bb} (at a distance of 10 kpc) of the radiating object during the flare, respectively. The triangles in **e** and **f** represent the temperature and the radius corrected for scattering effects (see Sect. 5.2). The horizontal lines in **e** indicate the time intervals for which spectra are shown in Fig. 2. The dashed line marks the time when the source sets behind the earth and the dotted line the time when the source is below 145 km above the earth limb (see Sect. 3).

the 3σ confidence level. This apparent inconsistency is, however, not unexpected (see Arabadjis & Bregman 1999). During earth-atmosphere entry the absorbing column was found to be $(6 \pm 4) \times 10^{22} \text{ cm}^{-2}$.

After the peak of the flare the temperature of the emitting object is decreasing. The radius plotted in Fig. 1f is that of a sphere with an area equal to that predicted by the black-body flux, assuming that the source is at a distance of 10 kpc and that the emission is isotropic. The

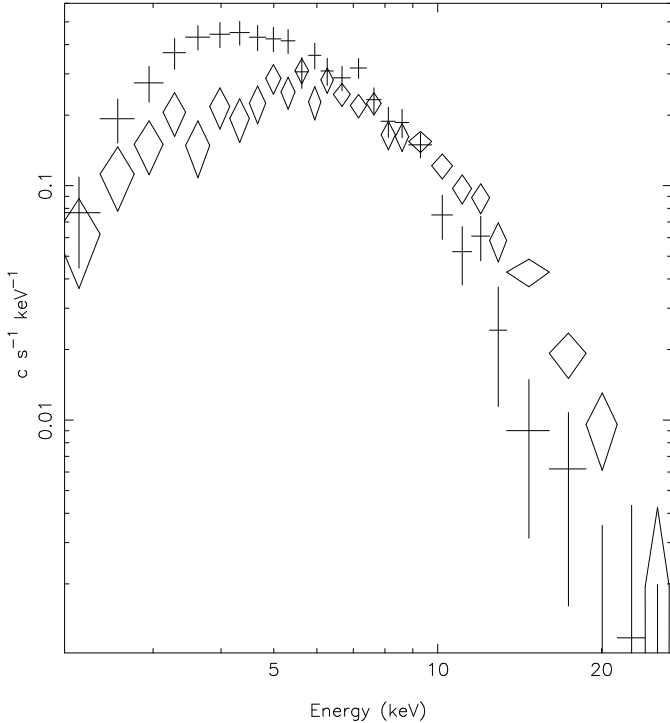


Fig. 2. Two examples of burst spectra from the time intervals indicated in Fig. 1e. The crosses indicate the first interval and the diamonds the second. The fitted blackbody temperatures are 1.63 ± 0.04 keV (crosses) and 2.38 ± 0.07 keV (diamonds).

radius peaks at the beginning of the burst, after which it starts to decrease, reaching a minimum after about 1 minute. It then increases again and levels off. There is a strong anti-correlation between the temperature and the black body radius.

5. Discussion

5.1. Physical Nature

Type-I X-ray bursts are believed to originate from thermonuclear flashes on the surfaces of neutron stars and have three main characteristics (see Lewin et al. 1993 for a review): 1) the shape is commonly described by a fast rise (< 10 s) and a longer exponential decay, 2) the spectrum is best described by a black-body model and 3) the spectrum shows softening during the decay phase (i.e. the neutron star photosphere cools). Some of the type-I bursts show evidence for photospheric radius expansion. The luminosity in such a burst becomes so high (i.e., reaches the Eddington limit) that the atmosphere of the neutron star expands due to radiation pressure. When the luminosity decreases below the Eddington limit, the atmosphere contracts again until it reaches the neutron star surface. During the expansion and contraction phases, the luminosity will stay close to the Eddington luminosity, because the excess luminosity is effectively transformed into kinetic

and potential energy of the atmosphere (Lewin et al. 1993, and references therein). The profiles of these bursts do not satisfy the first characteristic completely (fast rise and exponential decay): an Eddington-limited burst can show a period of almost constant flux after the rise, or a double peaked light curve. In extreme cases a brief precursor can be seen to the main event.

The flare from 1RXS J171824.2–402934 shows characteristics of an Eddington-limited type-I burst, see Fig. 1. The hardness (and equivalently the temperature) shows a peak in the beginning, corresponding to the start of the burst and a following decrease due to the expansion. When the atmosphere starts contracting, the temperature rises again, until the radius reaches its original value, after which the neutron star shows cooling, similar to type-I bursts. The initial rise and the following contraction can be seen in Fig. 1e. Surprisingly, the radius starts to increase again after it reaches a minimum value. This behavior is not unique and has been seen in other bursts (e.g. Tawara et al. 1984, Hoffman et al. 1980, Van Paradijs et al. 1990). The durations of those bursts were also long (> 60 s). A possible explanation is the deviation of the spectra from that of true black-body radiation. This will be discussed in Sect. 5.2.

If the burst is indeed Eddington-limited, it is possible to derive the distance. The Eddington luminosity L_{Edd} for $1.4 M_{\odot}$ neutron stars is about 2.0×10^{38} erg s^{-1} . Note that there is an uncertainty in this number because of the uncertainties in the composition (and therefore the opacity) and the mass of the neutron star. By making L_{Edd} equivalent to the observed flux we find a distance of 6.5 ± 0.5 kpc, assuming that the burst emission is isotropic, that the black-body temperature corresponds to the effective temperature and taking into account gravitational redshift effects.

Instead of the theoretical value for L_{Edd} we can use the observed peak luminosity of Eddington-limited bursts seen in globular clusters, for which the distances are known. This peak luminosity is 3.0×10^{38} erg s^{-1} (Lewin et al. 1993). From this we find a distance of about 8 kpc. It is clear that our distance determination to 1RXS J171824.2–402934 is a rough estimate.

Assuming a distance of 6.5 kpc, the total energy emitted in the burst is $\gtrsim 2.3 \times 10^{40}$ erg. If the energy released per gram in the nuclear fusion is between 1.6×10^{18} erg g^{-1} and 6×10^{18} erg g^{-1} (Lewin et al. 1995), a mass of at least 3.8×10^{21} g accreted material is involved. The persistent emission is quite uncertain, but if the level is lower than the maximum ROSAT value, 1×10^{-11} erg $\text{cm}^{-2} \text{s}^{-1}$, the time needed to accumulate 3.8×10^{21} g is at least 150 days. From the WFC upper limit we infer that the waiting time is at least 26 days. It is no surprise that no other bursts have been seen from this source at all.

The relatively low persistent emission can also explain the long duration of the burst. At very low accretion rates, the flashing layer is expected to be hydrogen rich (Fuji-

moto et al. 1981), and because of the long time scales involved in proton-capture processes, bursts are expected to last longer. Observations confirm this anti-correlation between low accretion rate and burst duration from a variety of burst sources (Van Paradijs et al. 1988).

All known type-I X-ray bursters that have identified optical counterparts are low-mass X-ray binaries (LMXBs, e.g., Van Paradijs 1995). In analogy, it is very likely that 1RXS J171824.2–402934 is a LMXB as well. Given the high level of Galactic absorption (predicting a severe optical extinction of $A_V \sim 18$) and the relatively large distance, it is difficult to find an optical counterpart.

5.2. Non-Planckian Spectra

In reality, X-ray bursts are not true black-body emitters. The spectra resemble Planckian functions, but the colour temperatures derived from these spectra are generally substantially higher than the true effective temperatures (Van Paradijs et al. 1990, and references therein). The reason is that electron scattering dominates the opacity at high temperatures, causing the photons to be Comptonized to higher energies. This has been confirmed by detailed modelling of neutron star atmospheres (e.g. London et al. 1984, 1986, Ebisuzaki 1987, Foster et al. 1986). These calculations show that the ratio of colour temperature to effective temperature depends mainly on the ratio of the luminosity to the Eddington luminosity. The dependency on other parameters such as surface gravity and chemical composition is very weak (see Lewin et al. 1993, and references therein).

To evaluate the magnitude of this effect in our burst, we made a correction using analytical fits from Ebisuzaki and Nakamura (1988) to the numerical results from Ebisuzaki (1987). According to these fits the colour temperature can be twice as high as the effective temperature if the luminosity is close to the Eddington luminosity. The corrected temperature and radius are also shown in Fig. 1. We assumed a hydrogen-rich composition ($X = 0.73$). It can be seen that the radius now increases a factor of ~ 1.6 after the minimum, i.e. less than the original increase (a factor of ~ 2).

Observations indicate that close to the Eddington limit the spectral hardening may be even larger than suggested above (see Lewin et al. 1993). If this is true, the increase of the radius will be even less than the factor 1.6 derived above.

We verified the above theoretical approach by an empirical approach obtained by Sztajno et al. (1985) from analysis of the source 4U 1636-53 and find similar results for $kT \lesssim 2$ keV.

6. Conclusion

We have discovered an Eddington-limited thermonuclear burst from the ROSAT source 1RXS J171824.2–402934.

In analogy with other X-ray bursters, this identifies this already-suspected X-ray binary as a low-mass X-ray binary with a neutron star. From equivalence of the peak flux and the Eddington luminosity, we find a distance of 6.5 kpc. ROSAT over the years detected variable low-level persistent 0.1-2.4 keV X-ray emission from this source which at maximum, given the distance, translates to a 0.1-2.4 keV luminosity of 10^{35} erg s $^{-1}$. No persistent emission was detected just before and after the burst above an upper limit which is one order of magnitude larger than the ROSAT measurements made several years prior to the burst.

Acknowledgements. We thank Jaap Schuurmans and Gerrit Wiersma for WFC software and data archival support. Paolo Soffitta is acknowledged for his work on the earth atmosphere absorption model. The data reported here were obtained during the Science Performance Verification phase. The BepoSAX satellite is a joint Italian and Dutch program. This research has made use of the Simbad database, operated at CDS, Strasbourg, France, of data obtained through the High Energy Astrophysics Science Archive Research Center Online Service, provided by the NASA/Goddard Space Flight Center, and of the ROSAT Data Archive of the Max-Planck-Institut für extraterrestrische Physik (MPE) at Garching, Germany.

References

- Arabadjis, J.S., Bregman, J.N., 1999, ApJ, 510, 806
- Boella, G., Butler, R.C., Perola, G.C., et al., 1997, A&A, 122, 299
- Dickey, J.M., Lockman, F.J., 1990, ARA&A, 28, 215
- Ebisuzaki, T., 1987, PASJ, 39, 287
- Ebisuzaki, T., Nakamura, N., 1988, ApJ, 328, 251
- Foster, A.J., Ross, R.R., Fabian, A. C., 1986, MNRAS, 221, 409
- Fujimoto, M.Y., Hanawa, T., Miyaji, S., 1981, ApJ, 247, 267
- Hoffman, J.A., Cominsky, L., Lewin, W.H.G., 1980, ApJ, 240, L27
- Jager, R., Mels, W.A., Brinkman, A.C., et al., 1997, A&A, 125, 557
- Lewin, W.H.G., van Paradijs, J. & Taam, R.E., 1993, Space Sci. Rev., 62, 223
- Lewin, W.H.G., van Paradijs, J. & Taam, R.E., 1995, in “X-ray binaries”, eds. W.H.G. Lewin, J. v. Paradijs, E.P.J. van den Heuvel, CUP, 175
- London, R.A., Taam, R.E. & Howard, M.W., 1984, ApJ, 287, L27
- London, R.A., Taam, R.E. & Howard, M.W., 1986, ApJ, 306, 170
- Motch, C., Guillout, P., Haberl, F., et al., 1998, A&A, 132, 341
- Sztajno, M., van Paradijs, J., Lewin, W. H. G., et al., 1985, ApJ, 299, 487
- Tawara, Y., Kii, T., Hayakawa, S., et al., 1984, ApJ, 276, L41
- Van Paradijs, J., Penninx, W., Lewin, W.H.G., 1988, MNRAS, 233, 437
- Van Paradijs, J., Dotani, T., Tanaka, Y., Tsuru, T., 1990, PASJ, 42, 633
- Van Paradijs, J., 1995, in “X-ray binaries”, eds. W.H.G. Lewin, J. v. Paradijs, E.P.J. van den Heuvel, CUP, 536

Voges, W., Aschenbach, B., Boller, Th., et al., 1999, *A&A*, 349,
389